

Electrical conductivity and percolation threshold of hybrid carbon/polymer composites

Atieh Motaghi,¹ Andrew Hrymak,¹ Ghodratollah Hashemi Motlagh²

¹Department of Chemical & Biochemical Engineering, Western University, London, Ontario N6A 5B9, Canada

²Department of Chemical Engineering, Faculty of Engineering, University of Tehran, Tehran, Iran 14395/1311

Correspondence to: A. Hrymak (E-mail: ahrymak@uwo.ca)

ABSTRACT: The electrical conductivity and percolation threshold of single and hybrid carbon filled composites are experimentally investigated. Polystyrene, carbon fiber (CF) and carbon black (CB) at three CF/CB ratios of 1.67, 3.33, 6.67 were compounded in a twin screw extruder micro-compounder and compression molded into sheets. The through-plane and in-plane electrical conductivity of the composites are measured by 2 and 4 probe techniques. The percolation threshold of the single filler and hybrid composites are determined from the experimental results using a percolation model. The hybrid composites have a higher value of electrical conductivity and lower percolation threshold than the single CF filler composite except for the CF/CB ratio of 6.67. The percolation threshold for the cases of single filler and hybrid composites are modeled. The hard core / soft shell model is used and it is assumed that the percolation in a particle filled system depends on the ratio of tunneling distance to particle diameter. This ratio is determined by modeling single filler composites using the experimental data and kept constant in the modeling of the hybrid system. Finite size scaling is used to determine the percolation threshold for the infinite size hybrid system containing (nanosize) particles and micron size fibers for three CF/CB ratios. The simulation results show that the percolations of hybrid composites have the same trends observed in the experimental results. © 2014 Wiley Periodicals, Inc. *J. Appl. Polym. Sci.* **2015**, *132*, 41744.

KEYWORDS: conducting polymers; polystyrene; theory and modeling; thermoplastics

Received 4 August 2014; accepted 7 November 2014

DOI: 10.1002/app.41744

INTRODUCTION

Most polymers are inherently electrically insulating. The electrical conductivity of polymers can be increased by the addition of conductive fillers.¹ Electrically conductive particles usually randomly distribute within an insulating matrix, and thus the entire composite may be insulating or electrically conducting depending on the percolation threshold, where the critical amount of conducting particles for the onset of electrical conduction is reached and the electrical properties of the material typically exhibit a non-linear behavior.²

The resulting conductive composites can substitute metals in some application such as electromagnetic shielding, and are light weight, and corrosion resistant thus lending themselves for special applications.^{3–5}

The electrical conductivity of composite materials has been modeled by several approaches for low or high content conductive fillers. However, most existing models are not able to predict the sharp transition in electrical conductivity.^{6–9}

Many attempts have been made to reduce the amount of filler by varying matrix type and filler size, shape and conductivity.

Recently, combination of two types of conductive fillers has promoted the formation of a conductive network for transferring charge within the insulating matrix.^{10–13}

At present, it seems there is insufficient knowledge about the physics of electrically networks of fillers in the polymeric material. To address the question of how to control the percolating network, percolation formulations in two- and three-dimensional systems for several types of lattice and continuum models (including circles, squares, sticks, spheres, and hemispheres) were first explored by Pike and Seager¹⁴ Moreover, Berhan and Sastry¹⁵ proposed a more realistic model by investigating the percolation threshold of systems of three-dimensional straight spherocylinders, which are randomly oriented within a unit cube using both hard-core and soft-core models.¹⁵ The soft core spherocylinder model erroneously supposes the fibers can merge, which can be significant even for very high aspect ratio fibers. The hard core spherocylinder model supposes the hard impenetrable core in fibers. Based on the excluded volume concept, it was found the percolation threshold is strongly dependent on the ratio of hard core to the soft shell rather than on the aspect ratio of fibers themselves.

Table I. Properties of PS

Property	Unit	Value
MFI (200°C/5 Kg)	g/10 min	11
Density	g/cm ³	1.04
Vicat softening point	°C	89.5
Tensile strength @ break	MPa	45
Elongation @ break	%	2
Tensile modulus	MPa	3100
Water absorption	%	<0.1

Table II. Properties of Carbon Fillers

Property	CB	CF
Electrical conductivity (S/cm)	10–100	625
Specific gravity	1.8	1.78
Bulk density (Kg/m ³)	100–120	360
Aggregate size (nm)	30–100	-
Pore volume (DBP, mL/100g)	480–510	-
Surface area (m ² /g)	1250	1.1
Fiber diameter (μm)	-	7.5
Fiber length (μm)	-	5000

In systems where the conducting particles are not in physical contact and tunneling is the dominant charge transport mechanism, the hard core with soft shell model is more suitable for modeling electrical percolation provided fiber geometry, fiber distribution, and the tunneling distance are known.⁴ Determining the tunneling distance experimentally is a complicated problem and geometry, orientation and ratio of fillers showed a significant effect on the percolation threshold.^{4,10,16,17}

Polymer composites containing carbon black (CB) show a uniform electrical conductivity and low percolation threshold

because of high surface area. However, high loading CB systems are not easily processed by extrusion due to the high viscosity. On the other hand, carbon fiber (CF) filled composites have a higher percolation threshold compared to CB systems. So, a large amount of CF is needed to achieve a conductive composite, as compared to CB systems, and a CF molten material also shows high shear viscosities for extrusion. Therefore, a combination of two fillers is one way to maximize the conductivity, while maintaining processability.

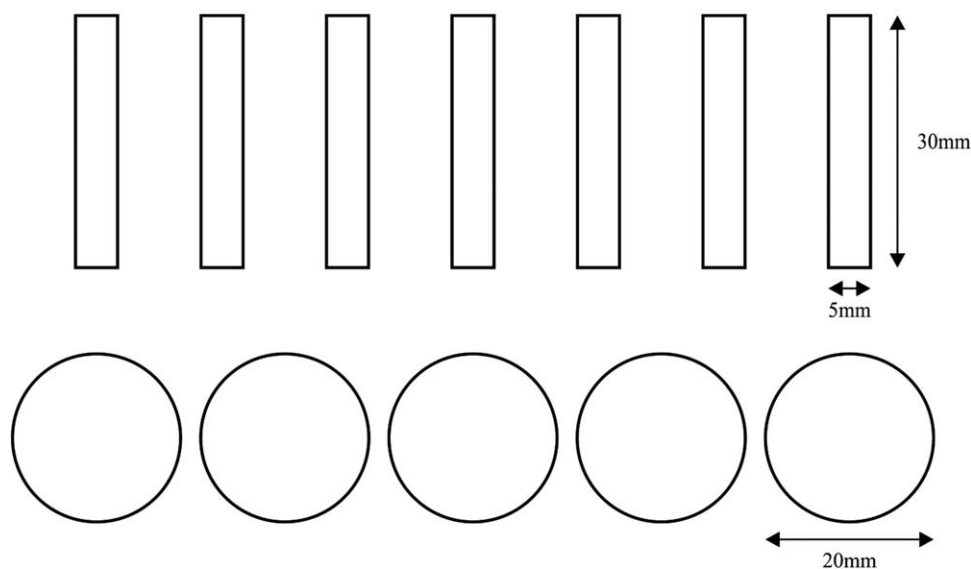
In this work, electrical conductivity and percolation of single filler and hybrid composites are studied over a wide range of filler content, accompanied by simulation of the percolation threshold in the hybrid composites. The hard core/soft shell model was used and the average fiber length and particle diameter were obtained from experimental analysis. Soft shell thicknesses (or tunneling distances) were determined from comparing the simulation of single filler composite with the experimental percolation threshold. Computer simulation provides the opportunity to manipulate the loading of fillers to achieve a percolation threshold and conductivity with minimal filler loading.

EXPERIMENTAL

Material

The thermoplastic matrix, polystyrene (PS), GPPS 1540, with a MFI of 11 g/10 min at 200°C, 5 Kg was obtained from Tabriz Petrochemical Company (Table I). Thermoplastic PS has a wide range of applications because of high chemical resistance, extremely low moisture absorption, and weathering resistance.

The two carbon fillers used in this study included PAN-derived chopped long CF, AGM94, 5 mm long and 7.5 μm in diameter, from Asbury Carbons and high surface area CB, Ketjenblack EC600JD, with aggregate size of 30–100 nm and surface area of 1250 m² g⁻¹ from Akzo Nobel. Table II shows the properties of the carbon fillers.

**Figure 1.** Cutting pattern for bars and disks shape samples.

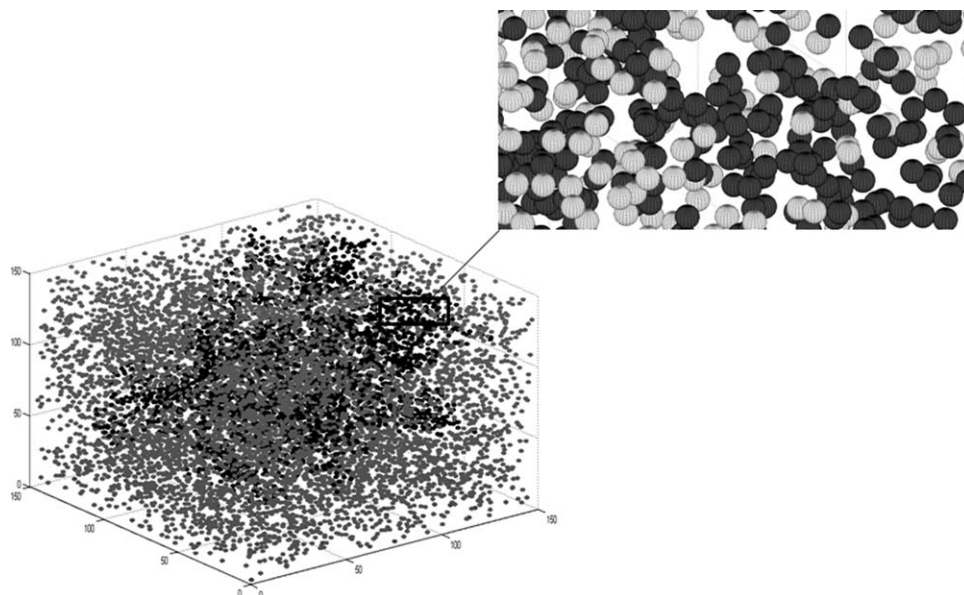


Figure 2. Cubic system of particles. ($D_p/\delta_p = 2$, cubic size = 150 nm).

Procedure

PS with various amounts of single CB, CF and two carbon fillers at three CF/CB ratios of 1.67, 3.33, and 6.6 was compounded in a twin screw micro-compounder, Haake Minilab Rheomix CTWS. All compounds were processed at 200°C for

about 7–10 min with the screw speed of 50–60 rpm. Maximum upper limit of temperature, minimum screw speed and optimum time were set to minimize the fiber breakage in the process. A sheet mold of 10 cm × 10 cm × 2.5 mm was used for compression molding of the compounds. The hot mold was

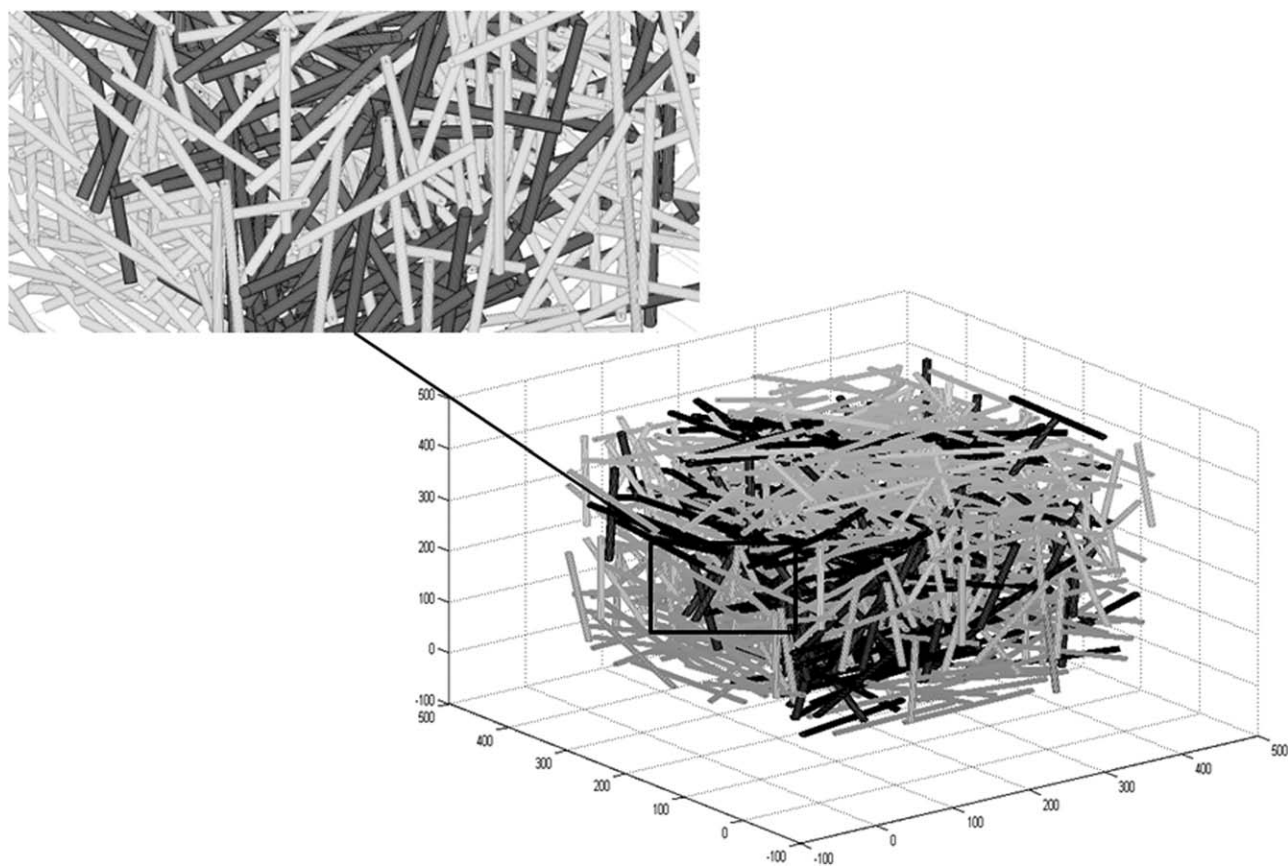


Figure 3. Cubic system of fibers. ($l/D_f = 21$, $\delta_f = 1.2 \mu$, cubic size = 450 μ).

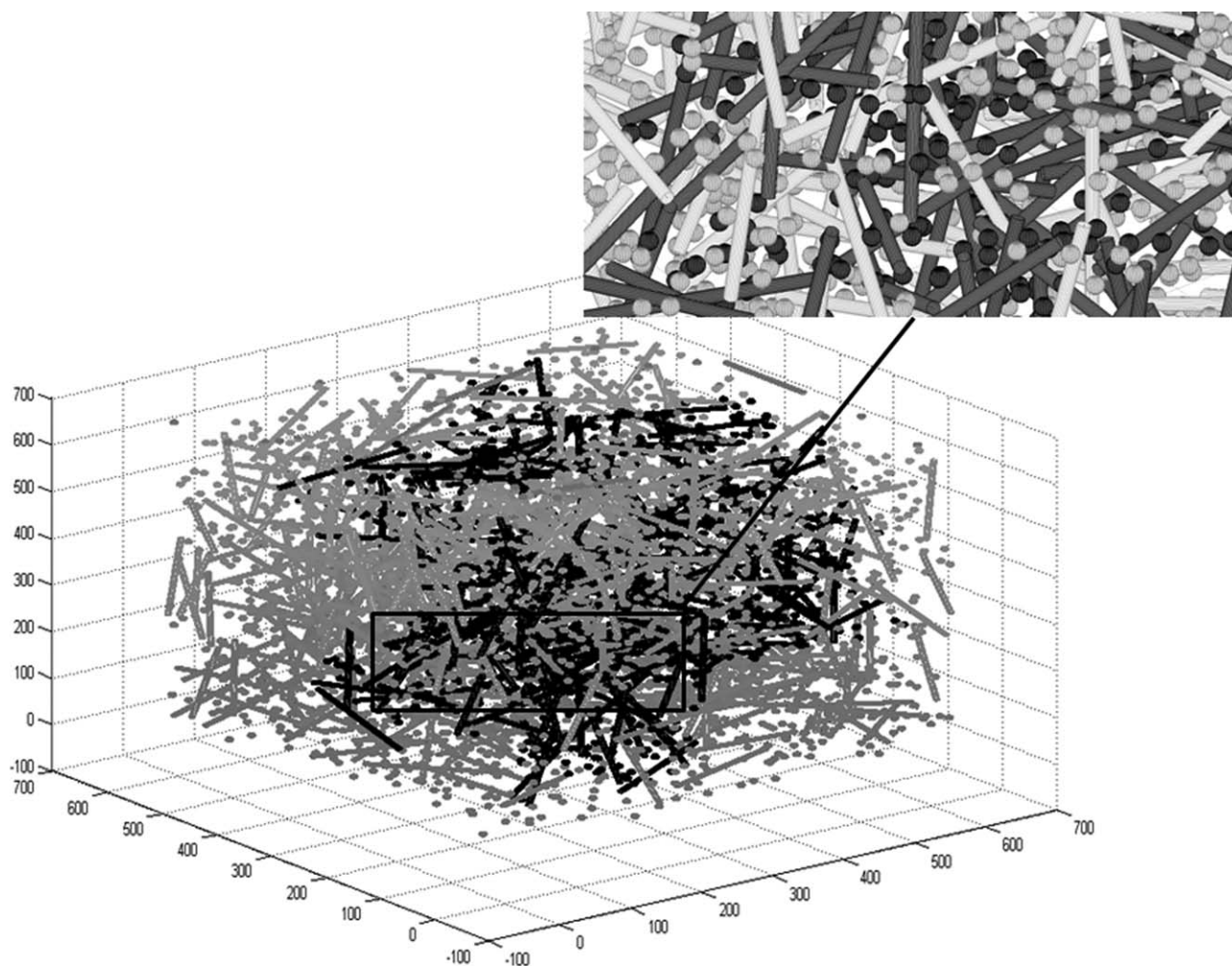


Figure 4. Cubic system of fibers and particles ($l/D_f=21$, $\delta_f=1.2 \mu$, $D_p/\delta_p=2$, cube size = 650μ , CF/CB = 1.67).

filled with the required amount of the compound at temperature of 220°C for 5 min as preheating stage to be certain of compound melting and reduce the orientation of fibers. A pressure of 8000 psi was applied for 3 min by hydraulic press. The mold was cooled by cold water and the sheet was removed and cut to small bars of 30×5 mm and disks of 2 cm diameter according to the pattern shown in Figure 1 for further analysis.

Analysis

Electrical conductivity was measured by 2-probe and 4-probe method for through plane and in plane direction.^{10,18,19} In the 4 probe method, the bar sample was placed between the two copper electrodes and depending on the sample resistivity the voltage of 2, 5, 10, and 30 volt was applied by power supply (BK1670A). The minimum voltage was used to prevent the heat generation in each sample. Then, the voltage was measured by the two probes of a voltmeter (Tektronix CDM250) on the surface of the samples at 20 mm distance for at least six samples. The current was read from the power supply. In the 2-probe method, the disk shape sample was placed between the two copper electrodes. Copper paper and applied pressure were used to minimize the contact resistance between the copper electrodes and surfaces of the sample. A voltage of 2 or 5 volt was applied

and the current was read. Both methods were set from the previous work.¹⁰ For samples with low conductivity (below the order of 10^{-10} S/cm), a high resistance meter (Keithly 600B)

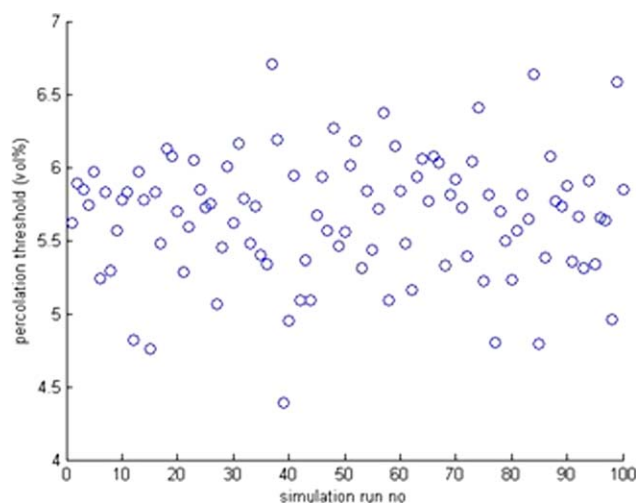


Figure 5. Percolation threshold for each run ($l/D_f=21$, $\delta_f=1.2$ and cube size = 450). [Color figure can be viewed in the online issue, which is available at wileyonlinelibrary.com.]

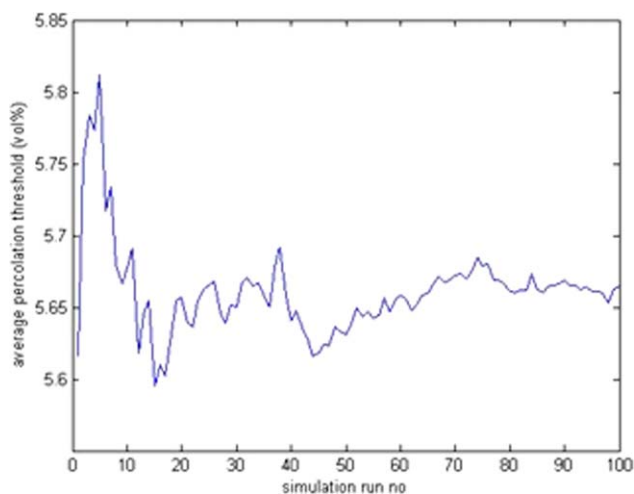


Figure 6. Average percolation threshold after each run ($l/D_f=21$, $\delta_f=1.2$ and cube size = 450). [Color figure can be viewed in the online issue, which is available at wileyonlinelibrary.com.]

was used to measure the resistance in both 2-probe and 4-probe methods.

To measure the fiber length distribution, samples were ashed in a furnace at 550°C for 15 min to burn out the polymer. The remaining fibers were collected, dispersed in ethanol, and spread over a microscopic slide to observe them under an optical microscope for taking images. The lengths of fibers were measured by using Image Pro Plus 7.0 for about 1000 fibers for each sample. The mean fiber length was calculated for composite of 5, 10, 15 vol % CF and hybrid composite of 10 vol % CF, 3 vol % CB.

To quantify the orientation of CF in the molded composites, bar samples were mounted in epoxy resin. Then the cross section was polished with different types of sand paper from SIC 800 to 4000 to reach the best quality of the surface. Digital images were taken from the polished surfaces and analyzed with Image Pro Plus 7.0. The analysis was done for at least 1000 fibers in each cross section to obtain the average radiuses of the fibers (a , b) and the angle to the axis (α).¹⁹

The average in-plane angles (α) were directly calculated from the obtained values. The average out-plane angles (β) were obtained from the eq. (1).

$$\beta = \sin^{-1}(b/a) \quad (1)$$

Then the 3D orientation factors were calculated according to the following expressions;

$$f_L = \frac{1}{n} \sum \cos^2 \alpha \cos^2 \beta \quad (2)$$

$$f_W = \frac{1}{n} \sum \sin^2 \alpha \cos^2 \beta \quad (3)$$

$$f_T = \frac{1}{n} \sum \sin^2 \alpha \quad (4)$$

where L , W , and T represents the direction in length, width, and thickness of the sample, respectively. The orientation factors can only vary from 0 to 1. For a composite with random fiber orientation, $f_L=f_W=f_T=1/3$ and for a composite with completely unidirectional orientation in x direction $f_L=1$ and $f_W=f_T=0$.

Transmission electron microscopy (TEM) was used to visualize CB aggregate size and structure in the CB composite and the distribution of CB aggregates in the vicinity of CFs in the hybrid composites. To prepare the samples, a thin layer with a thickness of 70 nm was cut from the molded composites by a microtome machine. TEM was done for composite of 0.5 and 2.5 CB vol % and hybrid composite of CF6.6, CB 1 vol %, and CF10, CB3 vol %. The average CB aggregate size was calculated considering at least 80 aggregates of the single CB composites.

SIMULATION

The percolation threshold was modeled using the random sequential method (RSA).²⁰ A number of particles or fibers were distributed randomly in a cube. Using the hard core-soft shell model, the cluster was formed by overlapping the regions in the space of the cube and the percolation threshold was reported as a volume fraction of particles/fibers in the cube.

Procedure

CB composites were considered as a dispersed system containing spherical particles. The particles were considered as hard core concentric spheres with diameter of D_p and soft shell thickness of δ_p . In the fiber filled composites, fibers were considered as hard core of concentric cylinders with length of l , diameter of D_f and soft shell thickness of δ_f . The hard core represented the actual fiber or particle which was impenetrable and soft shells were the penetrable part of fiber or particle, and represented the maximum tunneling distance for two neighbors to be regarded to be in electrical contact. The geometry used for the simulation was a cubic box as a control volume to create a composite with random distribution of objects. Depending on the type of filler in composite, particle, fiber or both of them, the conductive objects were randomly placed into the cube with the constraint that hard cores could not go through each other. Two particles were connected if the distance between the centers was less than $2(D_p + \delta_p)$ and greater than $2(D_p)$. In the case of fibers, they were regarded as connected if the soft shells overlapped considering the three different patterns of connectivity, body to body, end to body, and end to end.⁴ In the hybrid composite, fibers and particles were placed in the cube depending on the fiber to particle ratio. In such a composite, in addition to connectivity of only fibers and only particles, particles and fibers were connected if the soft shells penetrate each other. The number of objects was

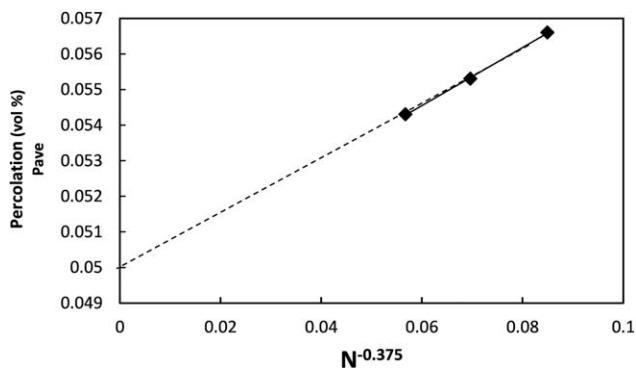


Figure 7. Percolation threshold as a function of $N^{-0.375}$ ($l/D_f=21$, $\delta_f=1.2$).

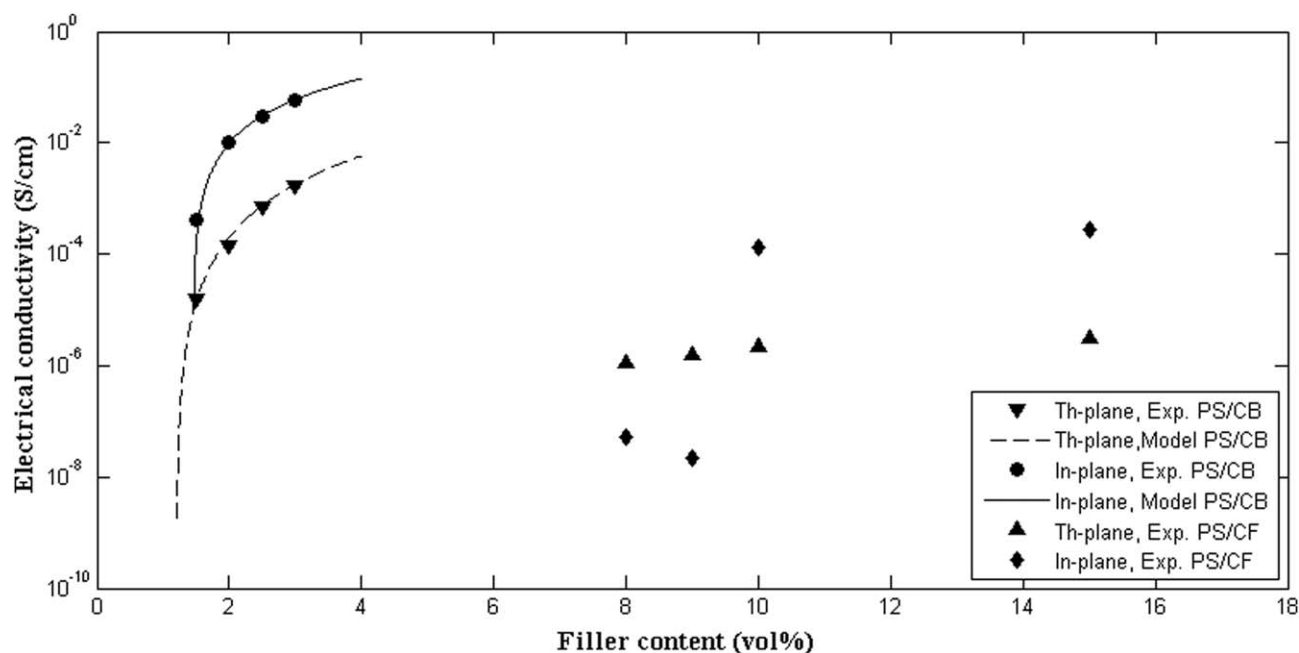


Figure 8. In-plane and through plane electrical conductivity of PS/CB and PS/CF composite.

continually increased and all the possible modes of connectivity were checked until a cluster of connected fibers/particles span all sides of cube. Figures 2–4 show the composites created by this procedure.

The output of the percolation simulation with RSA method in a finite system depends on the cube size due to the statistical nature of the onset of percolation. Every time that simulation runs, a particular sequence of random fibers generates to reach the percolation threshold. Therefore, every simulation run gives a different percolation threshold. Figure 5 shows the percolation threshold for CF with $l/D_f=21$ and $\delta_f=1.2$ and cube size of 450 for each run. The average percolation threshold for each cube size was obtained from running many simulations with different particle arrays to converge a constant average number. Figure 6 shows average percolation threshold (P_{ave}) after each run.

Using finite size scaling, the percolation threshold for the infinite system is obtained from eq. (5).^{2,4}

$$|P_{ave} - P_c| = N^{-0.375} \quad (5)$$

where P_{ave} is average percolation threshold of a finite-sized system (certain cube size), P_c is percolation threshold in an infinitely large system, and N is number of percolated objects in the system. Percolated objects can be fibers, particles, or both in a finite-sized sys-

Table III. Percolation Model Eq. (6) Parameters for PS/CB and PS/CF Compounds

	In plane		Through plane	
	PS/CF	PS/CB	PS/CF	PS/CB
σ_f (S/cm)	10	87	11	90
φ_{crit} (vol %)	5	1.45	5	1.2
t	4.5	1.75	5	2.7

tem. For calculation of P_c , the average percolation threshold volume fraction (P_{ave}) was plotted as a function of $N^{-0.375}$ for different size systems (Figure 7). By extrapolating the P_{ave} versus $N^{-0.375}$ straight line to the y -axis (where N approaches infinity), the intercept yields the percolation threshold (P_c) for the infinite system. For the composite shown in Figure 7, the percolation threshold was estimated at 5 vol %. Extracting the tunneling distance (soft shell thickness) is a complicated phenomena. For this work, soft shell thickness of single filler composite was adjusted to match the experimental percolation threshold and further used to predict the percolation threshold in hybrid composites.

RESULTS AND DISCUSSION

Experimental

Figure 8 shows the in-plane and through-plane electrical conductivity of PS/CB and PS/CF compounds in which the trend is similar to the findings by others.^{10,11,21–23} The electrical conductivity of PS/CB composites in both in-plane and through-plane directions shows an abrupt increase at much lower filler content as compared to PS/CF composites. The high structure CB aggregates with high surface area develop a high number of conductive paths at the nanoscale compared to micron size CF part. Figure 8 also shows that the in-plane conductivity is significantly higher than the through-plane conductivity. The induced preferred orientation of both CB and CF particles during the molding process can be the cause for the observed anisotropy.¹⁰

The percolation model describes the relation between composite conductivity and conductive filler concentration in the vicinity of and above the percolation threshold.

$$\sigma_c = \sigma_f (\varphi_f - \varphi_{crit})^t \quad (6)$$

where σ_c is composite conductivity (S/cm), σ_f is filler conductivity, φ_f is filler volume fraction ($\varphi_f > \varphi_{crit}$), φ_{crit} is percolation threshold and t is critical exponent. The values of σ_f , φ_{crit} ,

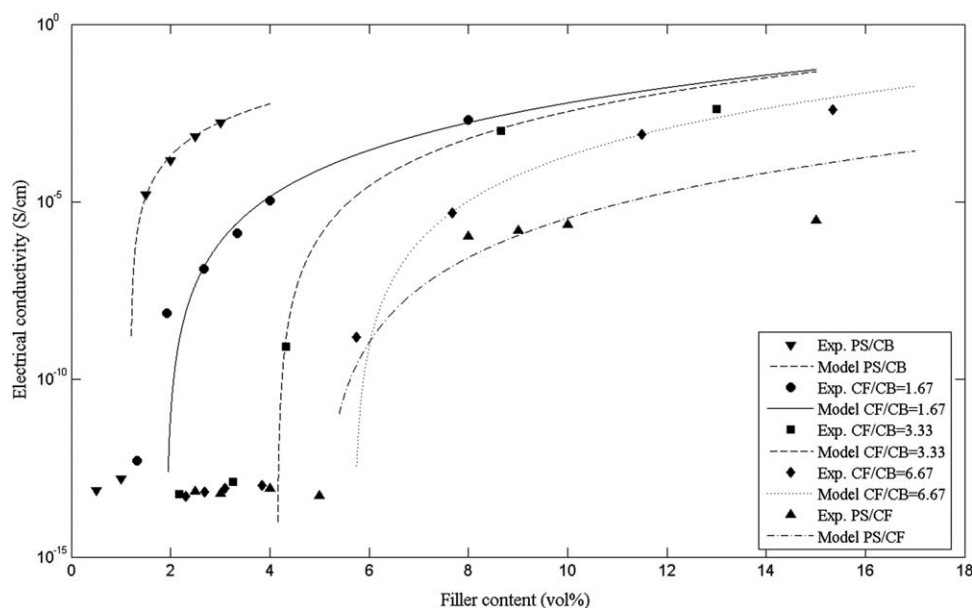


Figure 9. Through plane electrical conductivity of hybrid composite (with different ratios of CF/CB) compared to PS/CB and PS/CF compounds.

and t given in Table III were determined by fitting the experimental data points to eq. (6). The estimated values of φ_c and t for PS/CB compound are in good agreement with similar findings for high structure CB polymeric composites.^{1,7,22,24} The difference in φ_{crit} in PS/CF can be attributed to the CF aspect ratio and orientation, which is highly affected by the molding and compounding process.

Through plane electrical conductivity for the hybrid composite with different ratios of CF/CB, PS/CB and PS/CF compounds is illustrated in Figure 9. In hybrid composite lower content of filler is needed to make whole composite conductive comparing to PS/CF. The electrical conductivity of all hybrid composite is higher than PS/CF. The presence of CB in a PS/CF composite decreases the percolation threshold and increases the electrical conductivity. The CB effectively contributed to the establishment of the conductive paths between CFs.^{10,25} Percolation thresholds for hybrid composite are 1.9, 4.15, and 5.69 vol% for CF/CB ratios of 1.67, 3.33, and 6.67, respectively, estimated using the percolation model. The percolation threshold of the hybrid composite with the ratio of 6.67 is higher than PS/CF compound and may be due to CF breakage.

The changes in average CF length for PS/CF with 5, 10, and 15 vol % and PS/CF-CB with 10 vol % of CF and 3 vol % of CB are shown in Table IV. The results show that fiber breakage

Table IV. CF Length Analysis for Different PS/CF Compounds

Vol %	Fiber length (μ)	STD
CF5	235	133
CF10	162	73
CF15	124	68
CF10CB3	101	49

increases with an increase in fiber content because of the fiber-fiber collisions in the high shear twin screw extruder.^{10,25} The presence of CB in the melt has caused more fiber damage and it could be because of high viscosity, and the small size of extruder, where the interaction and collision of CB and CF increased.²⁵

Table V summarizes the orientation angles and factors for different PS/CF compounds. It can be seen that no significant differences were noted for different CF and CB content. A high value of α confirms that most of the fibers lied in the LW plane. Since f_T is smaller than f_L and f_W in most cases, this is confirming that fibers are preferentially oriented in the plane rather than out of plane.

The improved electrical conductivity due to CB is mainly attributed to the contribution of CB and CF in formation of conductive pathways.^{10,26} TEM image for PS/CB with 2.5 vol % (above percolation threshold) is illustrated in Figure 10. Most of the aggregates in the PS/CB composite have a linear “L” shape. The average size of the main structure is 196 nm. Also TEM images of hybrid composite show that CB has a uniform distribution around CF.

SIMULATION

Particle Composite Simulation

Percolation threshold is determined at the particle concentration such that the overlapped particles span. Table VI shows the

Table V. Fiber Orientation Angles and Factors in Three Principle Directions (L , W , and T)

Vol %	Average β ($^\circ$)	Average α ($^\circ$)	f_L	f_W	f_T
CF5	16	70	0.14	0.74	0.1
CF10	27	66	0.18	0.6	0.22
CF15	17	58	0.28	0.61	0.11
CF10 CB1.5	20	64	0.2	0.66	0.14

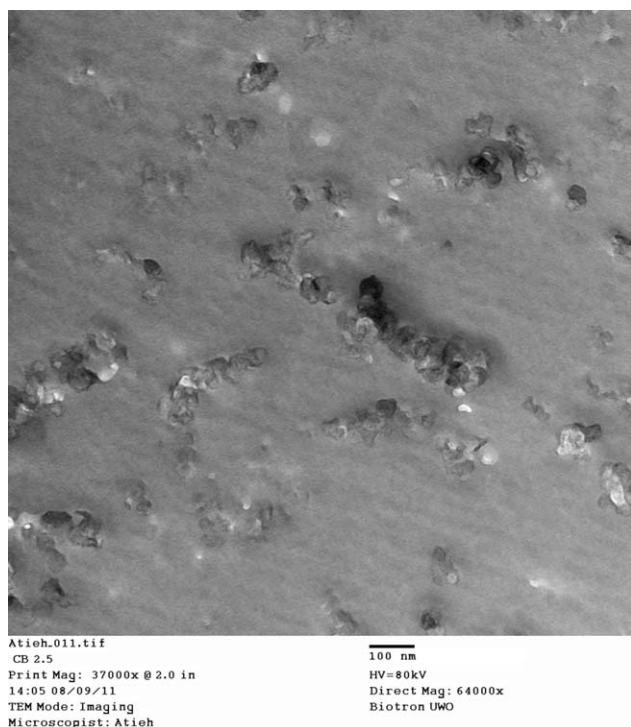


Figure 10. TEM image of PS/CB with 2.5 vol %.

system summarized for the percolation threshold for low structure CB filled composite. Results from simulation are in a good agreement with previous findings.¹⁷ For a CB filled composite, the smaller the radius of particles, the lower the percolation threshold. Also, the smaller the tunneling distance, the higher the percolation threshold.

Figure 11 illustrates the percolation threshold as a function of ratio of particle diameter to tunneling distance. Percolation thresholds from simulation have a good agreement with findings by other researchers.²⁷ Percolation for particulate composites strongly depends on the ratio of tunneling distance to radius rather than particle size alone.

Hybrid Composite Simulation

For the simulation of hybrid composites, fibers and particles were randomly placed in the system according to ratio of CF/CB (1.67, 3.33, and 6.67). Because of different CF length at vari-

Table VI. Percolation Threshold for Low Structure CB

Input data		Output (percolation threshold volume fraction)	
Radius ¹⁷ (μ)	Tunneling distance ¹⁷ (μ)	From simulation	Data ¹⁷
0.15	0.01	0.33	0.35
0.16	0.008	-	0.4
0.045	0.009	0.2	0.2
0.075	0.01	0.25	0.25
0.125	0.007	0.34	0.37

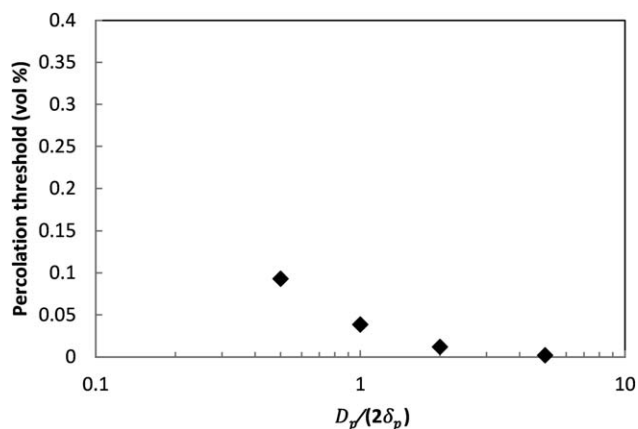


Figure 11. Percolation threshold as a function of particle diameter to tunneling distance.

ous loadings of filler in single and hybrid composites, two l/D_f of 21 and 15 were used. The tunneling distance of 1.2 μm for fibers, the same as CF composite, were used. To meet the experimental percolation threshold for CB composite (1.2 vol %), the ratio of $\frac{D_p}{\delta_p} = 2$ and this value was used for modeling of the hybrid composites. MATLAB R2010b saved the coordination locations of CF and CB in matrices. The size of CB, nm, was much smaller than the size of CF, μm , in the hybrid system. The simulation box requires the order of 10^{14} of CB particles and MATLAB exceeded the sufficient memory for storage matrix to save CB locations. To overcome this problem, larger size particles with the same ratio of D_p/δ_p were used. Finite size scaling was applied to calculate the percolation for different ratios of CF/CB (1.67, 3.33, and 6.67).

The percolation thresholds for hybrid composite obtained were 1.88, 2.29, and 2.83 vol %, for hybrid composite with l/D_f of 21, for the ratios of CF/CB of 1.67, 3.33, and 6.67, respectively.

Figure 12 shows the percolation threshold as a function of ratio of CF volume content to the total volume filler content. By decreasing fiber length, the calculated percolation threshold approached the experimental result. The average CF length for a hybrid composite of CF10CB3 vol %, in which the total filler

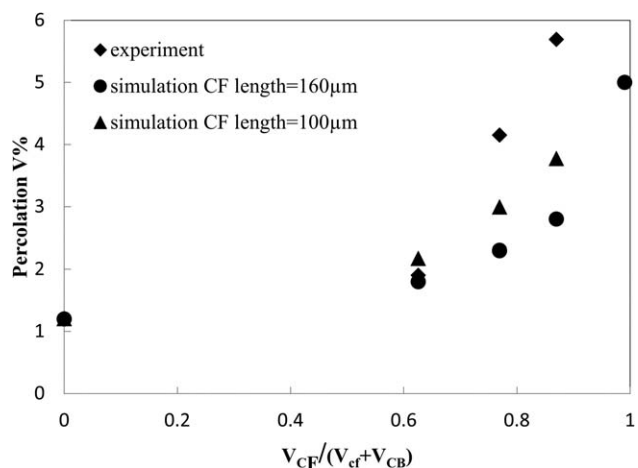


Figure 12. Percolation from experiment and simulation.

content is above the percolation threshold, was 101 μm as given in Table IV. By addition of CB to the hybrid composite at high CF content fiber breakage intensifies, which is the main reason for higher percolation threshold of hybrid composite of CF/CB ratio of 6.67 than CF single composite. CFs were preferably oriented in plane due to extrusion compounding and the addition of CB and CF was restricted by matrix due to viscous flow and small size of extrusion. In the simulation, the CF were randomly distributed and freely placed in the cube. CF had a length distribution due to breakage in the experimental work, while in the simulation the average length of CFs was used for all fibers. TEM results showed that CB have linear structure, a size distribution and may orient in the matrix. It may also be possible that CB particles have a tunneling distance distribution. These additional CB factors were not considered in this simulation.

CONCLUSIONS

The electrical conductivity of carbon filled PS samples was studied for CF and CB composites and three different ratios of CF/CB. It was observed that the combination of carbon fillers show higher electrical conductivity compared to CF composite, which is attributed to the CB in establishment of conductive pathways. For example, the addition of CB in hybrid composites increased the electrical conductivity for more than 3 orders of magnitude.

The percolation simulation of composites containing particles compared well with existing percolation models and experimental results in references. Percolation thresholds for hybrid composite calculated from computer simulation together with finite size scaling show the same trend as experimental results and give a good estimation of the experimental percolation threshold. The simulated percolation thresholds decrease with increase of amount of particles for all ratio of CF/CB.

REFERENCES

1. King, J. A.; Johnson, B. A.; Via, M. D.; Ciarkowski, C. J. *J. Appl. Polym. Sci.* **2009**, *112*, 425.
2. Sahimi, M. *Heterogeneous Materials I: Linear Transport and Optical Properties*; Springer Verlag: New York, **2003**.
3. Clingerman, M. L.; King, J. A.; Schulz, K. H.; Meyers, J. D. *J. Appl. Polym. Sci.* **2002**, *83*, 1341.
4. Ogale, A.; Wang, S. *Compos. Sci. Technol.* **1993**, *46*, 379.
5. Al-Ghamdi, A.; Al-Hartomy, O. A.; Al-Salamy, F.; Al-Ghamdi, A. A.; El-Mossalamy, E.; #Abdel Daiem, A.; El-Tantawy, F. *J. Appl. Polym. Sci.* **2012**, *125*, 2604.
6. Weber, M.; Kamal, M. R. *Polym. Compos.* **1997**, *18*, 711.
7. Balberg, I. *Carbon* **2002**, *40*, 139.
8. Schwartz, G.; #Cervený, S.; Marzocca, A. *Polymer* **2000**, *41*, 6589.
9. Cai, W.-Z.; #Tu, S.-T.; Gong, J.-M. *J. Compos. Mater.* **2006**, *40*, 2131.
10. Motlagh, G.; #Hrymak, A.; Thompson, M. *J. Polym. Sci. Part B: Polym. Phys.* **2007**, *45*, 1808.
11. Taipalus, R.; #Harmia, T.; #Zhang, M.; Friedrich, K. *Compos. Sci. Technol.* **2001**, *61*, 801.
12. King, J. A.; #Barton, R. L.; Hauser, R. A.; Keith, J. M. *Polym. Compos.* **2008**, *29*, 421.
13. Wei, T.; Song, L.; Zheng, C.; Wang, K.; Yan, J.; Shao, B.; Fan, Z.-J. *Mater. Lett.* **2010**, *64*, 2376.
14. Pike, G.; Seager, C. *Phys. Rev. B* **1974**, *10*, 1421.
15. Berhan, L.; Sastry, A. *Phys. Rev. E* **2007**, *75*, 041120.
16. White, S. I.; DiDonna, B. A.; Mu, M.; Lubensky, T. C.; Winey, K. I. *Phys. Rev. B* **2009**, *79*, 024301.
17. Ambrosetti, G.; Johnner, N.; Grimaldi, C.; Maeder, T.; Ryser, P.; Danani, A. *J. Appl. Phys.* **2009**, *106*, 016103.
18. Hashemi-Motlagh, G.; Thompson, M. R.; Hrymak, A. N. AICHE Annual Meeting, San Francisco, CA, November 12–17, **2006**.
19. Motlagh, G.; Hrymak, A.; Thompson, M. *Polym. Eng. Sci.* **2008**, *48*, 687.
20. Tarjus, G.; Schaaf, P.; Talbot, J. *J. Stat. Phys.* **1991**, *63*, 167.
21. Clingerman, M. L.; Weber, E. H.; King, J. A.; Schulz, K. H. *J. Appl. Polym. Sci.* **2003**, *88*, 2280.
22. Yuan, Q.; Wu, D. *J. Appl. Polym. Sci.* **2010**, *115*, 3527.
23. Tsotra, P.; Friedrich, K. *Compos. Part A: Appl. Sci. Manuf.* **2003**, *34*, 75.
24. Balberg, I. *Phys. Rev. Lett.* **1987**, *59*, 1305.
25. Drubetski, M.; Siegmann, A.; Narkis, M. *J. Mater. Sci.* **2007**, *42*, 1.
26. Sumfleth, J.; Adroher, X. C.; Schulte, K. *J. Mater. Sci.* **2009**, *44*, 3241.
27. Johnner, N.; Grimaldi, C.; Balberg, I.; Ryser, P. *Phys. Rev. B* **2008**, *77*, 174204.